

ADER schemes for the shallow water equations in channel with irregular bottom elevation

G. Vignoli*, V.A. Titarev⁺ and E.F. Toro⁺

**CISMA srl. c/o BIC Suedtirolo, via Siemens 19, Bolzano, Italy*

*⁺Laboratory of Applied Mathematics, Faculty of Engineering, University of
Trento, Trento, Italy*

Abstract

This paper deals with the construction of high-order ADER numerical schemes for solving the one-dimensional shallow water equations with variable bed elevation. The non-linear version of the schemes is based on ENO reconstructions. The governing equations are expressed in terms of total water height, instead of total water depth, and discharge. The ENO polynomial interpolation procedure is also applied to represent the variable bottom elevation. ADER schemes of up to fifth order of accuracy in space and time for the advection and source terms are implemented and systematically assessed, with particular attention to their convergence rates. Non-oscillatory results are obtained for discontinuous solutions both for the steady and unsteady cases. The resulting schemes can be applied to solve realistic problems characterized by non-uniform bottom geometries.

Key words: Shallow water; bottom variation; source terms, high-order methods, ENO, Godunov's method, derivative Riemann problem, ADER.

1 INTRODUCTION

There is a wide range of physical situations, such as flows in open channels and rivers, that can be mathematically represented by first-order non-linear systems of partial differential equations, whose derivation involves an assumption of the *shallow water type*. With rare exceptions, the governing equations are hyperbolic. The loss of hyperbolicity may occur in models of the multi-layer type, for which the equations are of mixed elliptic- hyperbolic type. Hyperbolicity and non-linearity mean that even for smooth initial conditions the solution may exhibit shock waves, or bores. Godunov-type methods, first developed in the aerospace industry to solve the compressible Euler equations, have steadily been exported to other application areas, including shallow water type flows. Early works in this direction are, for example, [25], [26], [9], [2], [7], [8]. An informative paper is [34], in which a large number of numerical methods for the one-dimensional shallow water equations are implemented and assessed. Further information on Godunov schemes for the shallow water equations is found in the textbook [27] and references therein.

Realistic shallow-water type models will include source terms, that is, non-differential terms that are functions of the vector of unknowns. For sometime it

has been accepted that the discretization of source terms can be as challenging as for the non-linear advection terms. It must be said that for most cases, even naive discretizations for source terms work reasonably well, but there are some well documented situations in which only sophisticated schemes can perform adequately. In the last decade there has been considerable progress on the development of special schemes to deal with source terms, amongst which the class of well-balanced schemes stands out, see for example [12,32,1].

When solving real problems one is likely to encounter all sorts of situations, with a high probability that naive schemes will compromise the quality and reliability of the solution.

Difficulties in discretizing source terms are present at the first order level. A separate issue is that of constructing schemes of higher order of accuracy. In view of Godunov's theorem [11], this is difficult even for equations without source terms, and schemes of second or higher order must necessarily be non-linear to avoid the production of unphysical oscillations in the vicinity of large spatial gradients. There are currently good second-order schemes for the shallow water equations, although it is sometimes difficult to ascertain whether the second-order of accuracy is valid for all the terms involved or not.

In this paper we study numerical methods that address these two difficulties, namely (i) source terms and (ii) high order of accuracy. There have been some works in this direction. For example, ENO and WENO methods have already

been applied to the shallow water equations; see for instance [4].

Here we are concerned with ADER type schemes. These methods were introduced in [29], where schemes of arbitrary accuracy were formulated for linear problems in one and multiple space dimensions. Corresponding schemes for non-linear systems are reported in [30], [22], [31], [24]. Further developments of ADER schemes are reported in [21], [18], [19], [17], [14], [15], [16], [6], [5].

The ADER methodology is a Godunov-type approach in which the numerical flux uses the solution of the so-called Derivative Riemann Problem (DRP) [30], [28]. In this type of Riemann problems the initial conditions consist of two variable vectors either side of the initial discontinuity, instead of two constant vectors, as in the classical Godunov method. In the solution of the intercell DRP to compute the numerical flux, the influence of the source term is included, that is, the numerical flux knows of the source term. Then the numerical source term is computed from a volume integral evaluated on high order solutions in space and time, within the space-time volume. In this manner ADER schemes of arbitrary order of accuracy for both the non-linear advection and the source terms can be constructed. Preliminary results on the ADER method for the shallow water equations are presented in [23], [31].

In this paper we report on ADER schemes based on ENO non-linear reconstructions for the shallow water equations with source terms due to bottom variation. The objective is to construct high-order, well-balanced non-

oscillatory schemes. Well-balanced schemes are constructed using (i) a suitable formulation of the governing equations and (ii) a staggered grid for the source terms. The free surface elevation and water discharge are defined at the centre of the volume, while the bottom elevation is defined at the volume interfaces. The source term and the numerical fluxes are then evaluated using the solution of the Derivative Riemann problem [30], [28]. The resulting ADER schemes are of arbitrary order of accuracy and are applicable to smooth and discontinuous solutions, both steady and unsteady.

The rest of the paper is as follows. Sect. 2 is about the governing equations and its reformulation. Section 3 describes the numerical methods of this paper. Numerical results are presented in section 4. In section 5 we perform a detailed convergence-rate study of the methods. Appendix A contains details of the Cauchy-Kowalewski procedure for the equations of this paper and Appendix B reports on convergence rates of the schemes for the model advection-reaction equation.

2 FORMULATION OF THE PROBLEM

The shallow water equations can be written in conservative form for the simple case of an horizontal bed channel and vanishing bottom friction in terms of

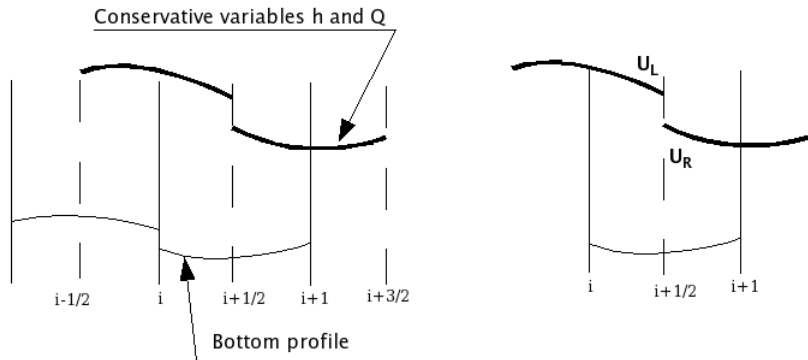


Fig. 1. Formulation of the problem, data reconstruction (left), control volume and Derivative Riemann problem (right).

the water depth D and water discharge Q in the following form [32,10]:

$$\begin{cases} \frac{\partial D}{\partial t} + \frac{\partial Q}{\partial x} = 0, \\ \frac{\partial Q}{\partial t} + \frac{\partial}{\partial x} \left(\frac{Q^2}{D} + \frac{1}{2}gD^2 \right) = -gD \frac{\partial b}{\partial x}, \end{cases} \quad (1)$$

where b is the bottom elevation, t and x are the temporal and spatial independent variables respectively, and g is the acceleration due to gravity. See Figure 1, where a longitudinal profile representing a couple of computational cells is depicted.

It is known that when the equations include source terms standard numerical schemes applied to (1) do not perform satisfactorily, particularly for the steady-state case. This is because only the relative position between the free surface and the bed profile is known and the information regarding the absolute position of the free surface (or of the bed) is lost. There are two physical situations of interest here; one in which the particle velocity is zero, which we call stationary flow, and one in which temporal partial derivatives in (1) are

identically zero, steady flow. Standard explicit schemes for the shallow water with source terms do not seem to converge to the exact solution in any of the two cases above.

In order to design a numerical method capable of reproducing both steady and unsteady solutions we follow the formulation of the equations reported in [33], using the free surface elevation $h = D + b$ as an unknown, with which (1) becomes:

$$\begin{cases} \frac{\partial h}{\partial t} + \frac{\partial Q}{\partial x} = 0, \\ \frac{\partial Q}{\partial t} + \frac{\partial}{\partial x} \left(\frac{Q^2}{h-b} + \frac{1}{2}gh^2 - gbh \right) = -gh \frac{\partial b}{\partial x}. \end{cases} \quad (2)$$

System (2) is hyperbolic with eigenvalues $\lambda^{(i)}$ and right eigenvectors $R^{(i)}$:

$$\lambda^{(1)} = u - a, \lambda^{(2)} = u + a, \quad \mathbf{R}^{(1)} = \begin{pmatrix} 1, \\ u - a \end{pmatrix}, \quad \mathbf{R}^{(2)} = \begin{pmatrix} 1 \\ u + a \end{pmatrix},$$

where $u = Q/D$ is the flow velocity and $a = \sqrt{gD}$ is the celerity.

The two main advantages of formulation (2) are that the model reproduces in the correct manner the physics of the problem, and it allows us to use existing Riemann solvers, such as the exact Riemann solver in [27], for the evaluation of the numerical fluxes between neighbouring computational volumes.

3 EQUATIONS AND NUMERICAL SCHEME

In this section we describe in detail our numerical methods for solving the shallow water equations with source terms in one space dimension.

3.1 Finite Volume Schemes

System (2) can be written in the following conservative form:

$$\frac{\partial \mathbf{U}}{\partial t} + \frac{\partial \mathbf{F}}{\partial x} = \mathbf{S} \quad (3)$$

where the unknown vector \mathbf{U} , the flux vector \mathbf{F} and the source term \mathbf{S} are given by

$$\mathbf{U} = \begin{pmatrix} h \\ Q \end{pmatrix}, \quad \mathbf{F} = \begin{pmatrix} Q \\ \frac{Q^2}{h-b} + \frac{1}{2}gh^2 - ghb \end{pmatrix}, \quad \mathbf{S} = \begin{pmatrix} 0 \\ -gh \frac{\partial b}{\partial x} \end{pmatrix}.$$

Integration of (3) over the control volume $I_i = [x_{i-\frac{1}{2}}, x_{i+\frac{1}{2}}] \times [t^n, t^{n+1}]$ on the $x - t$ plane gives:

$$\mathbf{U}_i^{n+1} = \mathbf{U}_i^n - \frac{\Delta t}{\Delta x} (\mathbf{F}_{i+\frac{1}{2}} - \mathbf{F}_{i-\frac{1}{2}}) + \Delta t \mathbf{S}_i. \quad (4)$$

Here \mathbf{U}_i^n is the cell average of the solution at time level t^n , $\mathbf{F}_{i+\frac{1}{2}}$ is the time average of the flux at cell interface $x_{i+\frac{1}{2}}$ and \mathbf{S}_i is the time-space average of the source term over the control volume, namely

$$\begin{aligned}\mathbf{U}_i^n &= \frac{1}{\Delta x} \int_{x_{i-\frac{1}{2}}}^{x_{i+\frac{1}{2}}} \mathbf{U}(t^n, x) dx, & \mathbf{F}_{i+\frac{1}{2}} &= \frac{1}{\Delta t} \int_{t^n}^{t^n+\Delta t} \mathbf{F}(x_{i+\frac{1}{2}}, t) dt, \\ \mathbf{S}_i &= \frac{1}{\Delta t \Delta x} \int_{t^n}^{t^n+\Delta t} \int_{x_{i-\frac{1}{2}}}^{x_{i+\frac{1}{2}}} \mathbf{S}(x, t) dx dt.\end{aligned}\tag{5}$$

3.2 The ADER Approach

In order to construct a numerical method for the solution of (3) we need to define suitable approximations to $\mathbf{F}_{i+\frac{1}{2}}$ and to \mathbf{S}_i , preserving the same notation, which are then called the *numerical flux* and the *numerical source*, respectively. We use the cell centred approach for the unknown vector \mathbf{U} , while for the bottom elevation, which appears in the formulation for the fluxes $\mathbf{F}_{i+\frac{1}{2}}$ and for the source terms \mathbf{S}_i , we use an interface-centred approach; the averaged values $b_{i+\frac{1}{2}}$ are defined as

$$b_{i+\frac{1}{2}} = \int_{x_i}^{x_{i+1}} b(x) dx .$$

In order to develop high-order numerical schemes we use the ADER approach for the evaluation of the numerical fluxes and of the numerical source. The ADER approach consists of three steps: i) reconstruction of high-degree polynomials starting from the cell average values of the solution; ii) solution of

the derivative Riemann problem and evaluation of the intercell flux $\mathbf{F}_{i+\frac{1}{2}}$;
 iii) evaluation of the numerical source \mathbf{S}_i by a high-order computation of the space-time integral inside the control volume.

Point-wise values of the solution at time level t^n are found from the reconstructed high-degree polynomials. In this paper we use the ENO [13,20] reconstruction procedure in order to avoid spurious oscillations, leading to a non-linear numerical scheme. We note that the reconstruction is performed both for the unknown vector \mathbf{U} and for the bottom elevation b (only once), as depicted in Figure 1.

After the data reconstruction procedure we solve the following Derivative Riemann Problem:

$$\partial_t \mathbf{U} + \partial_x \mathbf{F}(\mathbf{U}) = \mathbf{S}(\mathbf{U}),$$

$$\mathbf{U}(x, 0) = \begin{cases} \mathbf{p}_i(x), & x < x_{i+\frac{1}{2}}, \\ \mathbf{p}_{i+1}(x), & x > x_{i+\frac{1}{2}}, \end{cases} \quad (6)$$

to find the solution at $x = x_{i+\frac{1}{2}}$, denoted by $\mathbf{U}_{i+\frac{1}{2}}(\tau)$, where $\mathbf{p}_i(x)$ denotes the reconstructed polynomial in the i -th cell. Note that the value $b_{i+\frac{1}{2}}$ as well as its spatial derivatives are known. Following [30,28] we find the approximate flux at cell interface using an appropriate Gaussian rule:

$$\mathbf{F}_{i+\frac{1}{2}} = \sum_{\alpha=0}^N \mathbf{F}\left(\mathbf{U}_{i+\frac{1}{2}}(\gamma_\alpha \Delta t)\right) K_\alpha, \quad (7)$$

where γ_α are suitable Gaussian coefficients. The solution $\mathbf{U}_{i+\frac{1}{2}}(\tau)$ of the DRP problem (6) is found by first expressing it as a Taylor series expansion:

$$\mathbf{U}_{i+\frac{1}{2}}(\tau) = \mathbf{U}(x_{i+\frac{1}{2}}, 0^+) + \sum_{k=1}^{r-1} \left[\partial_t^{(k)} \mathbf{U}(x_{i+\frac{1}{2}}, 0^+) \frac{\tau^k}{k!} \right], \quad (8)$$

$$\partial_t^{(k)} \mathbf{U}(x_{i+\frac{1}{2}}, 0^+) = \frac{\partial^k}{\partial t^k} \mathbf{U}(x_{i+\frac{1}{2}}, 0^+),$$

where $0^+ = \lim_{t \rightarrow 0^+} t$. The leading term $\mathbf{U}(x_{i+\frac{1}{2}}, 0^+)$ is found by solving the classical Riemann problem with piecewise constant data:

$$\partial_t \mathbf{U} + \partial_x \mathbf{F}(\mathbf{U}) = \mathbf{0}, \quad \mathbf{U}(x, 0) = \begin{cases} \mathbf{p}_i(x_{i+\frac{1}{2}}), & x < x_{i+\frac{1}{2}}, \\ \mathbf{p}_{i+1}(x_{i+\frac{1}{2}}), & x > x_{i+\frac{1}{2}}, \end{cases} \quad (9)$$

and evaluating its solution at $(x - x_{i+\frac{1}{2}})/t = 0$. We call $\mathbf{U}(x_{i+\frac{1}{2}}, 0^+)$ the Godunov state, which in this paper is evaluated using the exact Riemann solver [27]. The remaining terms in (8) are computed by replacing all time derivatives $\partial_t^{(k)} \mathbf{U}(x_{i+\frac{1}{2}}, 0^+)$ by functions of spatial derivatives $\partial_x^{(l)} \mathbf{U}(x_{i+\frac{1}{2}}, 0^+)$ using the Cauchy-Kowalesky procedure. The unknown spatial derivatives at $t = 0^+$ are found from the following linearized Riemann problems:

$$\partial_t \left(\partial_x^{(k)} \mathbf{U} \right) + \mathbf{A} \left(\mathbf{U}(x_{i+\frac{1}{2}}, 0^+) \right) \partial_x \left(\partial_x^{(k)} \mathbf{U} \right) = \mathbf{0}, \quad \mathbf{A}(\mathbf{U}) = \frac{\partial \mathbf{F}}{\partial \mathbf{U}},$$

$$\partial_x^{(k)} \mathbf{U}(x, 0) = \begin{cases} d^{(k)} \mathbf{p}_i(x_{i+\frac{1}{2}}), & x < x_{i+\frac{1}{2}}, \\ d^{(k)} \mathbf{p}_{i+1}(x_{i+\frac{1}{2}}), & x > x_{i+\frac{1}{2}}, \end{cases} \quad (10)$$

where $\mathbf{A}(\mathbf{U})$ is the Jacobian of the system and the symbol $d^{(k)}$ denotes the k -th derivative respect to the independent variable x . The boundary extrapolated values are found using the polynomials $\mathbf{p}_i(x)$, $\mathbf{p}_{i+1}(x)$ obtained by the ENO reconstruction procedure.

To evaluate the second component of the source term we first perform integration by parts:

$$\begin{aligned} \mathbf{S}_i^{(2)} &= \frac{1}{\Delta t \Delta x} \int_0^{\Delta t} \int_{x_{i-\frac{1}{2}}}^{x_{i+\frac{1}{2}}} \left(-gh \frac{\partial b}{\partial x} \right) dx dt = \\ &= -\frac{g}{\Delta t} \int_0^{\Delta t} \left(hb|_{x_{i+\frac{1}{2}}} - hb|_{x_{i-\frac{1}{2}}} \right) dt + \frac{g}{\Delta t \Delta x} \int_0^{\Delta t} \int_{x_{i-\frac{1}{2}}}^{x_{i+\frac{1}{2}}} b \frac{\partial h}{\partial x} dx dt \end{aligned} \quad (11)$$

The first part is evaluated using suitable Gaussian points and a Taylor time expansion for the evaluation of $h(x_{i\pm\frac{1}{2}}, t)$. The second integral in (11) is approximated by a Gaussian integration rule:

$$\frac{g}{\Delta x \Delta t} \int_0^{\Delta t} \int_{x_{i-\frac{1}{2}}}^{x_{i+\frac{1}{2}}} b \frac{\partial h}{\partial x} dx dt = g \sum_{\alpha=1}^N \left[\sum_{l=1}^N \left(b(x_\alpha) \frac{\partial}{\partial x} h(x_\alpha, \tau_l) \right) K_l \right] K_\alpha. \quad (12)$$

We note that the evaluation of (12) is not necessary for the first order version of the scheme. The first component of the source term (i.e. the source for the continuity equation) is equal to zero. The integral (12) must be evaluated by splitting the space integral in two parts: $x_{i-\frac{1}{2}} - x_i$ and $x_i - x_{i+\frac{1}{2}}$, because for the bed elevation $b(x)$ we adopt the interface centred approach, and two

different reconstructed polynomials for $b(x)$ are given in the i -th cell.

3.3 Source Terms and the Conservative Property

It is obvious that the governing equations contain non-vanishing terms also in the case of steady flow. Under stationary conditions in the momentum equation, both the source term due to the bottom elevation $-gh\frac{\partial b}{\partial x}$ and the flux term due to hydrostatic pressure $\frac{1}{2}gh^2 - ghb$ are different from zero.

A numerical method capable of reproducing the exact solution under steady conditions is said to satisfy the \mathcal{C} -property; the method is said to satisfy the approximate \mathcal{C} -property if it is accurate up to the prescribed order when applied to a steady problem [32]. The stationary solution, characterized by vanishing velocities everywhere in the domain, is a subset of the steady solutions. If the numerical scheme reproduces the exact solution in this case (i.e. $h = \text{constant}$, $Q = u = 0$) it is said to satisfy the \mathcal{Z} -property. The scheme proposed in this paper satisfies the \mathcal{Z} -property and the approximate \mathcal{C} -property.

We note that when $h = h_0 = \text{constant}$, $Q = 0$ and $u = 0$ in the whole domain, the reconstructed values $\mathbf{p}_i(x)$ and $\mathbf{p}_{i+1}(x)$ are equal to $h = h_0$, $Q = 0$ at all the interfaces between numerical cells. Moreover, reconstructed values for all the spatial derivatives of h and Q are equal to zero. We can now compute the

numerical fluxes, following the situation defined in Figure (1):

$$\mathbf{F}_{i-\frac{1}{2}} = \begin{pmatrix} 0 \\ \frac{1}{2}gh_{i-\frac{1}{2}}^2 + gh_{i-\frac{1}{2}}b_{i-\frac{1}{2}} \end{pmatrix}, \quad \mathbf{F}_{i+\frac{1}{2}} = \begin{pmatrix} 0 \\ \frac{1}{2}gh_{i+\frac{1}{2}}^2 + gh_{i+\frac{1}{2}}b_{i+\frac{1}{2}} \end{pmatrix}$$

The source term is then evaluated using integration by parts, and recalling that the spatial derivative of the reconstructed variable h is zero:

$$\begin{aligned} \mathbf{S}_i^{(2)} &= -\frac{g}{\Delta x \Delta t} \int_{t^n}^{t^n+\Delta t} \int_{x_{i-\frac{1}{2}}}^{x_{i+\frac{1}{2}}} h \frac{\partial b}{\partial x} dx dt = \\ &= \frac{g}{\Delta t} \int_{t^n}^{t^n+\Delta t} (bh|_{x-\frac{1}{2}} - bh|_{x+\frac{1}{2}}) dt = g (bh|_{x-\frac{1}{2}} - bh|_{x+\frac{1}{2}}) \end{aligned} \tag{13}$$

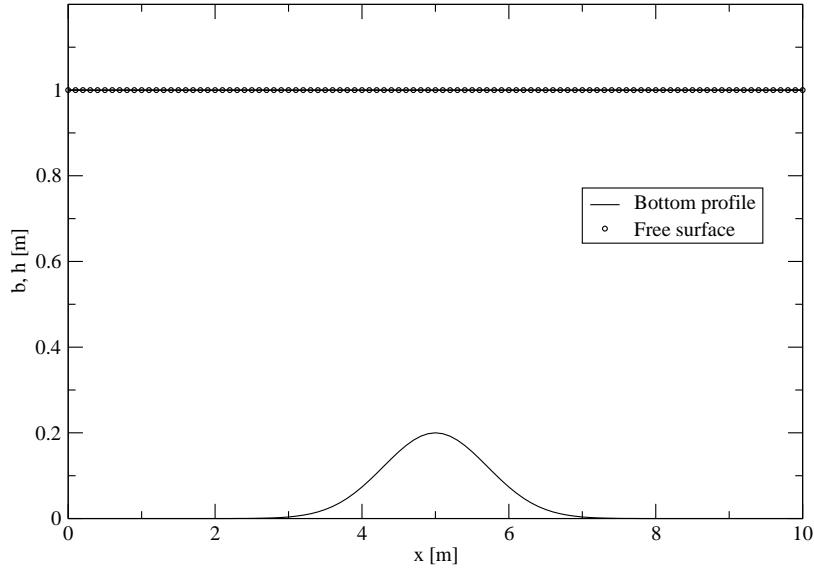


Fig. 2. Computed stationary state solution for the flow over a non horizontal bed with initial condition equal to $h = 1$ m, $Q = 0$ and $u = 0$.

Applying scheme (4) it is easy to show that the numerical scheme reproduces

the exact solution. The numerical results shown in Figure 2 verify the stated property of the scheme.

4 NUMERICAL SOLUTIONS

The numerical method is tested in order to verify that both steady and unsteady solutions are well reproduced. The latter case is traditionally associated with dam-break problems, characterized by the propagation of sharp fronts. In the former case both smooth and discontinuous solutions can be observed. Results reported in this paper are computed using Courant Number $CFL = 0.9$.

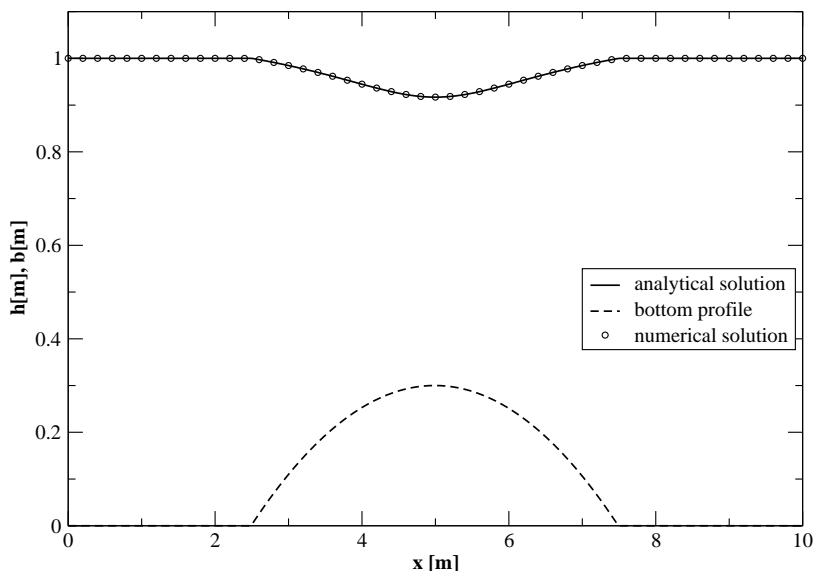


Fig. 3. Steady case: free surface elevation in the case of smooth solution and parabolic bed profile. ADER5 numerical method used. ($Q = 1m^3/s$, $b_{max} = 0.3m$, $h(x = L) = 1m$, $N = 50$, $L = 10m$).

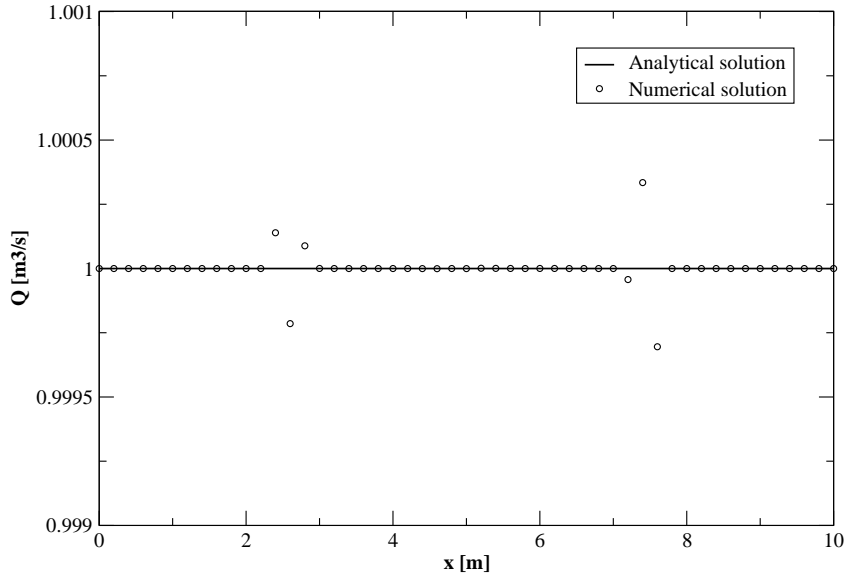


Fig. 4. Steady case: water discharge in the case of smooth solution and parabolic bed profile. ADER5 numerical method used. ($Q = 1\text{m}^3/\text{s}$, $b_{max} = 0.3\text{m}$, $h(x = L) = 1\text{m}$, $N = 50$, $L = 10\text{m}$). Note the scale for Q .

4.1 STEADY SOLUTIONS

For the test under steady conditions there are several different configurations characterized by smooth or discontinuous solutions, depending on the values of the water discharge Q , the maximum height of the bed profile b_{max} and the boundary conditions for the free surface elevation $h(x = 0)$ and $h(x = L)$, where L is the channel length. Figures 3 and 4 show the numerical results for free surface elevation and water discharge respectively, obtained with a fifth-order ADER method, for the standard test case of subcritical flow over a parabolic bump. This solution is computed using a maximum bed elevation sufficiently small such that the water flow remains subcritical over the numerical domain and the solution does not present discontinuities. This is the case

of the flow field in large rivers, where the irregular geometry produces small flow disturbances. The numerical method is able to reproduce the behaviour of the solution, the local flow acceleration and the perturbation of the free surface elevation.

Note that in Figure 4 the maximum error for the water discharge is very small.

For larger values of the elevation of the bump the free surface profile becomes steeper and steeper until it becomes discontinuous. This is the case reported in Figures 5 and 6, where the maximum bottom elevation is 0.5m. The numerical solution of Figures 5 and 6 agrees with the exact solution both for the free surface elevation and the water discharge.

We can notice that for the case of steady and discontinuous solutions, the position of the shock is stationary and depends on the water discharge, the maximum bottom elevation and on the boundary conditions. We remark that it is possible to obtain a better numerical solution (as plotted in the upper part of Figure 5) if we choose the spatial mesh in such a way that the shock is positioned exactly between two cells, in this case $N = 280$. Note that this procedure is not general because the position of the shock is not known *a priori*. In other words, for the steady shock solution the refinement of the computational grid does not always give more accurate results, as can be seen from Figures 5 and 6.

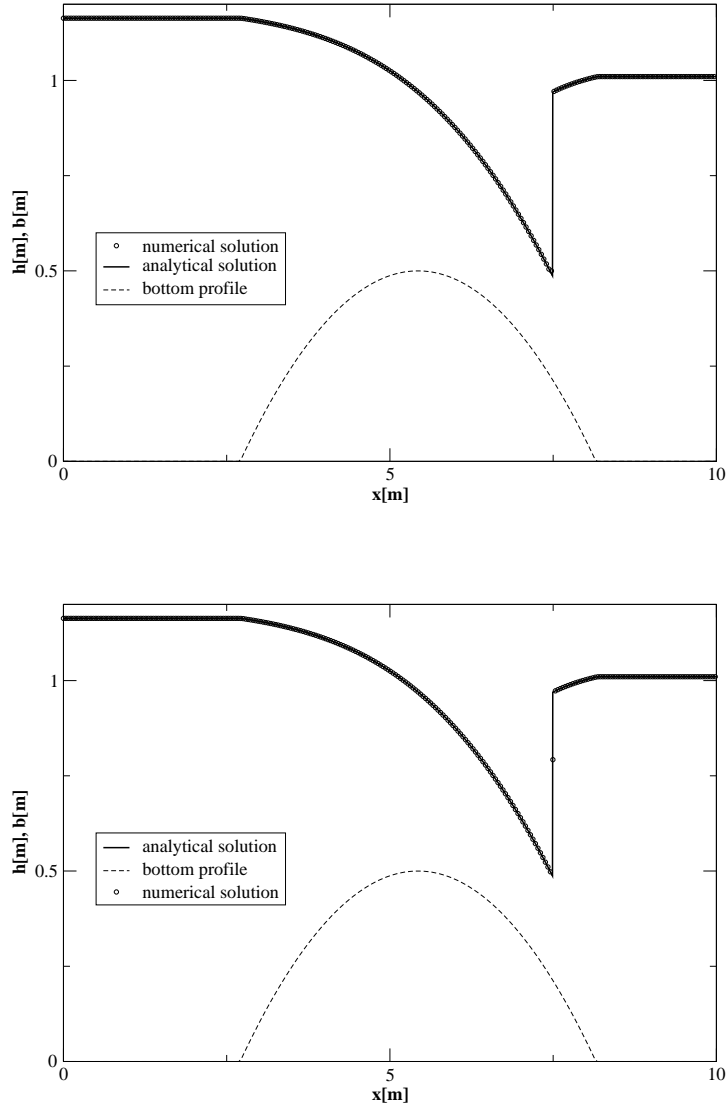


Fig. 5. Steady case: free surface elevation in the case of discontinuous solution and parabolic bed profile. ADER5 numerical method used. ($Q = 1m^3/s$, $b_{max} = 0.5m$, $h(x = L) = 1m$, top $N = 280$, bottom $N = 285$, $L = 10m$).

4.2 UNSTEADY SOLUTIONS

Unsteady solutions are the typical case for which in the past shock capturing numerical method have been constructed. In natural rivers and channels unsteady solutions with a low degree of temporal variability, like the flood wave,

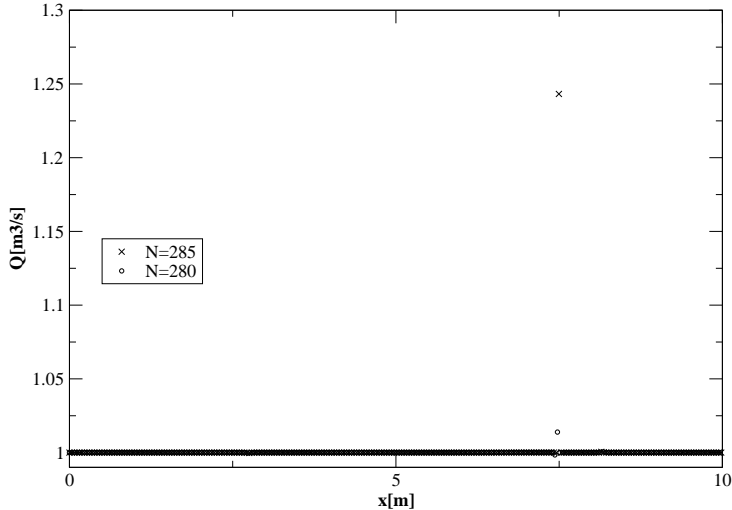


Fig. 6. Steady case: water discharge in the case of discontinuous solution and parabolic bed profile with two meshes $N = 280$ and $N = 285$. ADER5 numerical method used. ($Q = 1m^3/s$, $b_{max} = 0.5m$, $h(x = L) = 1m$, $L = 10m$).

are due to rainfall events. Rapid phenomena characterized by the formation of sharp fronts and bores are typically related to the presence of artificial structures. Finally sharp fronts and bores may occur in natural convergent estuaries during the propagation of tidal waves.

4.2.1 COMPARISON WITH THE EXACT UNSTEADY RIEMANN PROBLEM SOLUTION

Test cases under unsteady conditions are typically dam break problems. For this kind of problem the analytical solutions is available both for the case of horizontal bed profile and for the case of a step-like bottom. The first case has not been considered because in the case of an horizontal bottom profile our formulation reduces to the standard shallow water formulation. Instead we

consider a dam break problem over a step-like bottom profile, for which the exact solution is available [3]. The test considered has solution characterized by a right shock, by a stationary shock positioned in the central uniform zone of the flow field, between the rarefaction and the right moving shock. Figure 7 shows a comparison between the numerical solution obtained using an ADER3 scheme and the exact solution. Note that in the staggered grid setup of Figure 1, in the initial condition for the numerical solution the discontinuity for the free surface elevation and for the bottom profile are staggered by half a computational cell. In order to perform the comparison between numerical and analytical solutions we have used 500 computational cells, such that the space interval between the two discontinuities in the initial condition is sufficiently small. Good agreement is observed, results are essentially non-oscillatory for both shocks. The stationary shock in $x = 0 m$ is reproduced with a small error for the water discharge. As for the stationary test case, this error is due to the position of the numerical cell interface.

4.2.2 INITIAL DATA WITH A SMOOTH BED

As final example we report the numerical solution obtained for a dam break problem over a smooth bed profile. For this case the analytical solution is not available.

Results are reported in Figures 8 and 9 for the case of a Gaussian bed profile; under these conditions the solution displays two different shocks. The first one

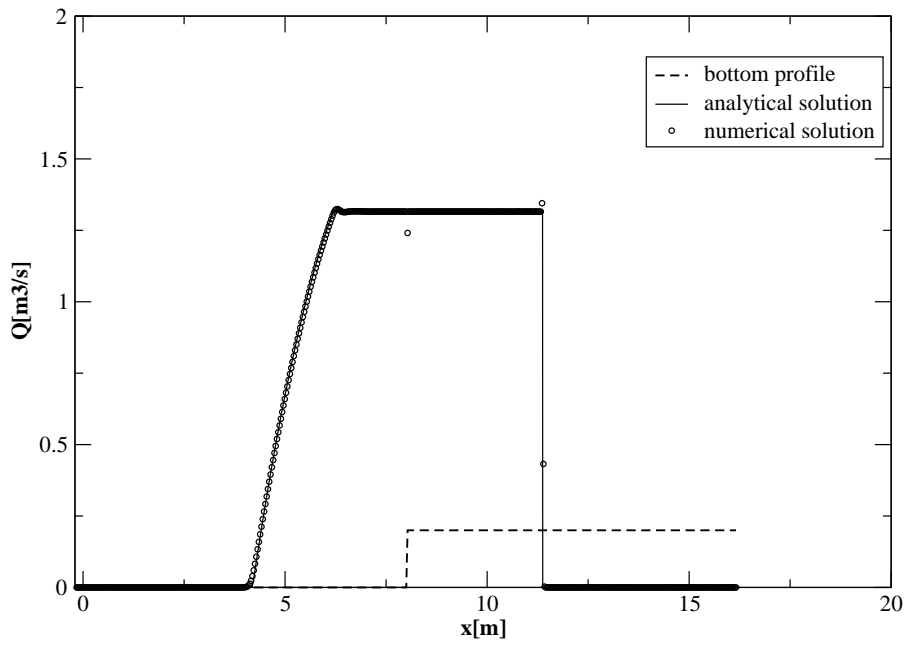
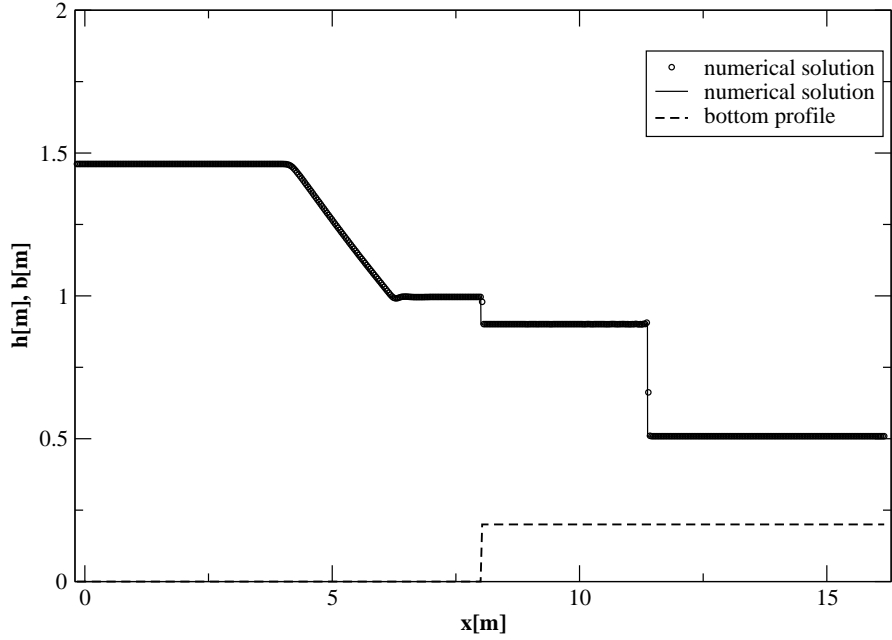


Fig. 7. Comparison between numerical and analytical solution for the dam-break problem with a bottom step. ADER 3 numerical method used. The initial conditions are $D_L = 1.461837m$, $D_R = 0.308732$ and $Q_L = Q_R = 0$, the step in the bottom profile is $0.2m$ high.

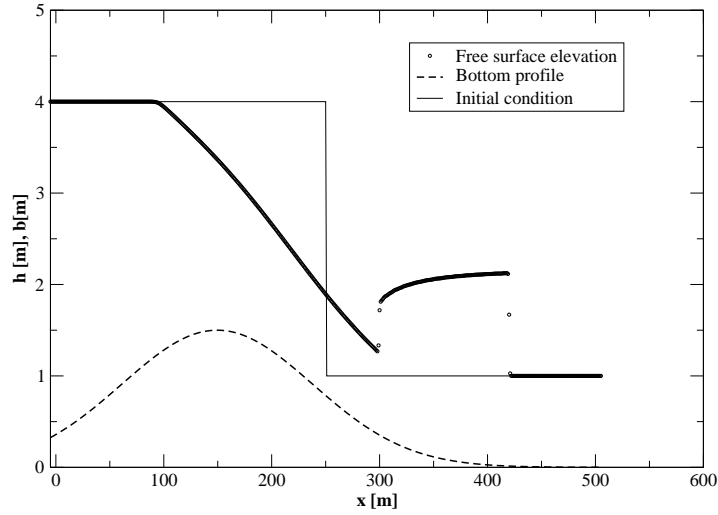


Fig. 8. Solution for dam break over a non horizontal profile. ADER3 numerical method used. The solution at time $t = 40s$ displays two shocks, $N = 500$ cells.

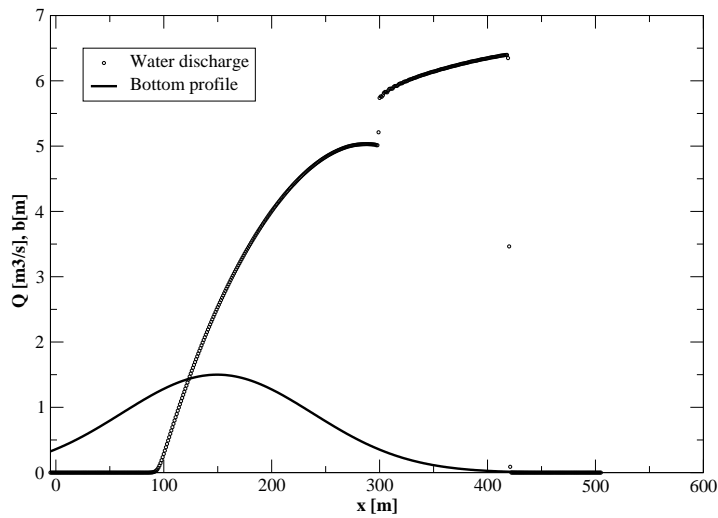


Fig. 9. Solution for dam break over a non horizontal profile. ADER3 numerical method used. The solution at time $t = 40s$ displays two shocks, $N = 500$ cells.

is due to the initial condition, the second appears in the middle region of the flow due to the bottom slope. The right shock propagates downstream and the second one is *quasi* stationary.

5 CONVERGENCE RATES STUDY

In the previous section we have shown that the proposed numerical methods reproduce both steady and unsteady solutions and the results are essentially non oscillatory. Here we measure the experimental order of accuracy of the schemes in order to verify that the theoretical order of accuracy is achieved. The accuracy of the schemes is measured both for the steady and the unsteady cases.

We have performed several tests using schemes up to 5-th order of accuracy both in space and in time; for all tests we use a Courant Number $CFL = 0.9$, the length of the numerical domain is 10 m and we use two different functions describing the bottom topography, namely a Gaussian function and a sinusoidal profile. Results with the sinusoidal bed profile are expected to be better than those obtained using a Gaussian bed profile. It is well known that in order to study the convergence rate of a scheme sinusoidal-type functions are preferable. In particular considering the simplest case of the model advection-reaction equation the theoretical orders of accuracy are reached by the numerical methods using a sinusoidal function, as shown in Appendix B.

In the non-linear shallow water case, considering the flow over a sinusoidal bed profile the free surface elevation $h(x, t)$ is a sinusoidal function only if the amplitude of the bottom elevation is small enough. For higher values of the maximum bottom elevation non-linearities in the governing equations give

rise to a more complex solution, characterized by larger values of the spatial derivatives of the solution $h(x, t)$. For larger values of the bottom elevation we obtain the limit case of discontinuous free surface profiles. Moreover, we notice that also for a sinusoidal free surface elevation the second component of the flux is not sinusoidal. All these considerations suggest that we should test the accuracy of the scheme, both for the steady and the unsteady cases, using small values for the sinusoidal amplitude of the bottom profile.

5.1 *STEADY CASE*

The numerical scheme is first tested under steady conditions, in order to verify that it satisfies the approximate \mathcal{C} -property.

The empirical rate of convergence of the schemes is tested for a Gaussian and for a sinusoidal bed profile. For the sinusoidal bed profile results are in agreement with the designed order of accuracy of the numerical scheme (see Tables 1 and 2) where we report the result obtained using two different amplitudes for the bed sinusoidal profile, 0.001 and 0.01 respectively. The prescribed orders of accuracy are well reproduced up to the fourth order scheme, whilst the fifth order scheme does not perform as expected, particularly, for the largest value of the bottom perturbation. As expected, for the Gaussian bed profile the achieved order of accuracy does not match the designed one, in particular for the ADER4 and ADER5 schemes (see Table 3). As expected,

Table 1

Convergence rates study for the steady and smooth case, sinusoidal bed profile
($b_{max} = 0.001m$, $Q = 1m^3s^{-1}$, $h(x = L) = 1m$)

Method	N	$L_1 error$	$L_1 order$	$L_\infty error$	$L_\infty order$
ADER 2	5	0.119E-03		0.252E-03	
	10	0.279E-04	2.09	0.610E-04	2.04
	20	0.616E-05	2.18	0.131E-04	2.21
	40	0.146E-06	2.07	0.297E-05	2.14
	80	0.357E-06	2.03	0.697E-06	2.09
ADER 3	5	0.501E-04		0.111E-03	
	10	0.783E-05	2.67	0.150E-04	2.89
	20	0.998E-06	2.97	0.201E-05	2.89
	40	0.128E-06	2.96	0.257E-06	2.97
	80	0.161E-07	2.98	0.323E-07	2.99
ADER 4	5	0.313E-04		0.703E-04	
	10	0.193E-05	4.02	0.451E-05	3.96
	20	0.114E-05	4.08	0.261E-06	4.10
	40	0.672E-08	4.08	0.150E-07	4.11
	80	0.414E-09	4.02	0.101E-08	3.88
ADER 5	5	0.138E-04		0.322E-04	
	10	0.603E-06	4.51	0.118E-05	4.76
	20	0.206E-07	4.87	0.408E-07	4.86
	40	0.903E-09	4.51	0.142E-08	4.84
	80	0.101E-09	3.15	0.185E-09	2.93

the fifth-order scheme is nevertheless the most accurate, errors are smaller.

5.2 UNSTEADY CASE

An exact solution to study the convergence rates is derived by prescribing two functions for $h(t, x)$ and $Q(t, x)$. Inserting these into system (2) produces a

Table 2

Convergence rates study for the steady and smooth case, sinusoidal bed profile
($b_{max} = 0.01m$, $Q = 1m^3s^{-1}$, $h(x = L) = 1m$)

Method	N	$L_1 error$	$L_1 order$	$L_\infty error$	$L_\infty order$
ADER 2	5	0.117E-02		0.248E-02	
	10	0.280E-03	2.06	0.606E-03	2.03
	20	0.617E-04	2.18	0.136E-03	2.15
	40	0.146E-04	2.07	0.309E-04	2.13
	80	0.358E-05	2.03	0.729E-05	2.08
ADER 3	5	0.489E-03		0.111E-02	
	10	0.769E-04	2.66	0.148E-03	2.90
	20	0.991E-05	2.95	0.200E-04	2.89
	40	0.128E-05	2.94	0.256E-05	2.96
	80	0.164E-06	2.96	0.323E-06	2.98
ADER 4	5	0.302E-03		0.685E-03	
	10	0.191E-04	3.98	0.440E-04	3.95
	20	0.119E-05	4.00	0.292E-05	3.91
	40	0.720E-07	4.05	0.223E-06	3.71
	80	0.916E-08	2.97	0.262E-07	3.08
ADER 5	5	0.131E-03		0.307E-03	
	10	0.602E-05	4.44	0.114E-04	4.74
	20	0.300E-06	4.32	0.510E-06	4.48
	40	0.386E-07	2.95	0.725E-07	2.81
	80	0.853E-08	2.18	0.169E-07	2.09

modified system with two source terms, the original one and a second term due to the fact that $h(x, t)$ and $Q(x, t)$ do not satisfy (2) but (14).

Table 3

Convergence rates study for the steady and smooth case, Gaussian bed profile
($b_{max} = 0.001m$, $Q = 1m^3s^{-1}$, $h(x = L) = 1m$)

Method	N	$L_1 error$	$L_1 order$	$L_\infty error$	$L_\infty order$
ADER 2	5	0.357E-04		0.971E-04	
	10	0.117E-04	1.60	0.286E-04	1.76
	20	0.304E-05	1.94	0.818E-05	1.80
	40	0.760E-06	2.00	0.212E-05	1.94
	80	0.189E-06	2.00	0.542E-06	1.96
ADER 3	5	0.249E-04		0.759E-04	
	10	0.386E-05	2.69	0.852E-05	3.15
	20	0.550E-06	2.80	0.114E-05	2.89
	40	0.764E-07	2.84	0.171E-06	2.74
	80	0.104E-07	2.86	0.337E-07	2.34
ADER 4	5	0.160E-04		0.454E-04	
	10	0.196E-05	3.02	0.468E-05	3.27
	20	0.307E-06	2.67	0.190E-05	1.30
	40	0.447E-07	2.78	0.268E-06	2.82
	80	0.512E-08	3.12	0.487E-07	2.46
ADER 5	5	0.131E-04		0.375E-04	
	10	0.894E-06	3.87	0.208E-05	4.16
	20	0.423E-06	1.07	0.347E-05	-0.78
	40	0.550E-07	2.94	0.687E-06	2.33
	80	0.533E-08	3.36	0.108E-06	2.66

The prescribed exact solution is:

$$h = h_0 + a_0 \sin\left(2\pi \frac{x}{L}\right) \cos\left(2\pi \frac{t}{T_0}\right),$$

$$Q = Q_0 - \frac{a_0 L}{T_0} \cos\left(2\pi \frac{x}{L}\right) \sin\left(2\pi \frac{t}{T_0}\right),$$

and the bottom elevation is:

$$b = b_0 \sin\left(2\pi \frac{x}{L}\right),$$

where L is the length of the computational domain and T_0 a suitable time period. The resulting artificial source term is evaluated numerically in the same way as the physical source term.

The "modified" equations read:

$$\begin{cases} \frac{\partial h}{\partial t} + \frac{\partial Q}{\partial x} = 0, \\ \frac{\partial Q}{\partial t} + \frac{\partial}{\partial x} \left(\frac{Q^2}{h-b} + \frac{1}{2}gh^2 - gbh \right) = -gh \frac{\partial b}{\partial x} + S(x, t). \end{cases} \quad (14)$$

The exact expression of the source term $S(x, t)$ is given by:

$$\begin{aligned} S(x, t) = & 4\pi \frac{a_0 \sin(\lambda x) \sin(\omega t) \left(Q_0 - \frac{a_0 L}{T_0} \sin(\omega t) \cos(\lambda x) \right)}{T_0 (h_0 + a_0 \cos(\omega t) \sin(\lambda x) - b_0 \sin(\lambda x))} - \\ & - \frac{2\pi \left(\frac{a_0}{L} \cos(\omega t) \cos(\lambda x) - \frac{b_0}{L} \cos(\lambda x) \right) \left(Q_0 - \frac{a_0 L}{T_0} \sin(\omega t) \cos(\lambda x) \right)^2}{(h_0 + a_0 \cos(\omega t) \sin(\lambda x) - b_0 \sin(\lambda x))^2} + \\ & + 2\pi g \frac{a_0}{L} \cos(\omega t) \cos(\lambda x) (h_0 + a_0 \cos(\omega t) \sin(\lambda x)) - \\ & - 2\pi g \frac{a_0 b_0}{L} \cos(\omega t) \cos(\lambda x) \sin(\lambda x) - 2\pi \frac{a_0 L}{T_0^2} \cos(\omega t) \cos(\lambda x) \end{aligned} \quad (15)$$

where $\lambda = \frac{2\pi}{L}$ and $\omega = \frac{2\pi}{T_0}$.

As for the steady case we have performed numerical tests using sufficiently

Table 4

Convergence rates study for the unsteady and smooth case, $b_0 = 0.001m$, $a_0 = 0.001m$, $Q_0 = 1m^3/s$, $T_0 = 10000s$

Method	N	$L_1 error$	$L_1 order$	$L_\infty error$	$L_\infty order$
ADER 2	5	0.152E-03		0.335E-03	
	10	0.391E-04	1.96	0.803E-04	2.06
	20	0.804E-05	2.28	0.180E-04	2.16
	40	0.182E-05	2.15	0.403E-05	2.16
	80	0.433E-06	2.07	0.951E-06	2.08
ADER 3	5	0.654E-04		0.126E-03	
	10	0.652E-05	3.33	0.150E-04	3.07
	20	0.103E-05	2.66	0.210E-05	2.83
	40	0.132E-06	2.96	0.269E-06	2.97
	80	0.163E-07	3.02	0.333E-07	3.01
ADER 4	5	0.381E-04		0.842E-04	
	10	0.267E-05	3.84	0.561E-05	3.91
	20	0.138E-06	4.27	0.306E-06	4.19
	40	0.718E-08	4.27	0.203E-07	3.91
	80	0.846E-09	3.09	0.207E-08	3.30
ADER 5	5	0.163E-04		0.377E-04	
	10	0.521E-06	4.97	0.118E-05	5.01
	20	0.159E-07	5.04	0.333E-07	5.16
	40	0.328E-08	2.28	0.463E-08	2.86
	80	0.909E-09	1.85	0.113E-08	2.03

small values for the amplitudes a_0 and b_0 , such that the non linearities appearing in the equations (in particular in the expression for the momentum flux) do not display a significant role. In Tables 5.2 and 5 we report the test case for $a_0 = 0.001m$, $b_0 = 0.001m$ and $a_0 = 0.01m$, $b_0 = 0.01m$ respectively. The prescribed order of accuracy is reached for the schemes up to fourth order, as for the steady test case. Difficulties are observed for the fifth order scheme

Table 5

Convergence rates study for the unsteady and smooth case, $b_0 = 0.01m$, $a_0 = 0.01m$, $Q_0 = 1m^3/s$, $T_0 = 10000s$

Method	N	$L_1 error$	$L_1 order$	$L_\infty error$	$L_\infty order$
ADER 2	5	0.152E-02		0.333E-02	
	10	0.389E-03	1.96	0.795E-03	2.06
	20	0.802E-04	2.27	0.180E-03	2.13
	40	0.181E-04	2.14	0.405E-04	2.15
	80	0.433E-05	2.06	0.946E-05	2.09
ADER 3	5	0.663E-03		0.125E-02	
	10	0.648E-04	3.35	0.149E-03	3.07
	20	0.102E-04	2.66	0.210E-04	2.82
	40	0.132E-05	2.95	0.271E-05	2.95
	80	0.164E-06	3.00	0.341E-06	2.98
ADER 4	5	0.372E-03		0.825E-03	
	10	0.277E-04	3.74	0.586E-04	3.81
	20	0.143E-05	4.27	0.311E-05	4.23
	40	0.841E-07	4.09	0.215E-06	3.85
	80	0.108E-07	2.95	0.223E-07	3.26
ADER 5	5	0.163E-03		0.374E-03	
	10	0.542E-05	4.91	0.125E-04	4.89
	20	0.203E-06	4.73	0.463E-06	4.76
	40	0.391E-07	2.37	0.630E-07	2.87
	80	0.103E-07	1.91	0.153E-07	2.03

even if it gives the smallest errors. This behaviour might be due to the nonlinearities in the equations; it does not seem to be related to the precision of the machine: tests using a quad-precision version of the code has been performed. In appendix B we report a test case for numerical schemes up to fifth order applied to the model advection-reaction equation. These tests are performed using the same numerical procedure and the same ENO reconstruction

as those adopted for the shallow water system. For the model equation the theoretical orders of accuracy are reached up to fifth order without difficulties (See Appendix B).

6 CONCLUSIONS

We have proposed a framework for constructing arbitrary high order numerical schemes for the solution of the shallow water equations with source terms. An important ingredient of the method is the high order reconstruction procedure. In this paper we have use the ENO method [13] instead of the more popular WENO approach [20]. The ENO technique has an important advantage in that the high order polynomial is known in the entire cell and its evaluation at all the Gaussian integration points is straightforward. The WENO technique on the other hand has some disadvantages in the presence of source terms. The evaluation of the source term and of the numerical fluxes requires the reconstructed values at a large number of points. In our approach the source term results from the evaluation of two integrals one to the left and one to the right. This means that one requires twice the number of WENO evaluation points, respect to approaches in which the source term is entirely defined within the cell. Moreover at one of these points, $b(x_{i\pm\frac{1}{2}})$, the WENO weights are negative. The second main ingredient of the technique is the solution of the Derivative Riemann Problem including source term.

We have systematically assessed the methods presented. The methods satisfy the \mathcal{Z} -property, that is, they produce the exact stationary solution for an horizontal free surface elevation and vanishing velocities. For the steady case the schemes are accurate up to the prescribed theoretical order and therefore they satisfy the approximate \mathcal{C} -property.

Steady solutions are well reproduced both in the smooth and in the discontinuous case. We note, however, that in the case of steady discontinuous solutions a refinement of the grid does not always give better results around discontinuities, except for the case when the discontinuity is aligned with a cell interface.

An important aspect of this paper is the high accuracy in space and time for hyperbolic systems with source terms. We have therefore paid a great deal of attention to the verification of the theoretical orders of accuracy of the schemes by empirical means. We have performed a study of the convergence rates of the schemes for which we have designed tests with small amplitude sinusoidal flows, both for the steady and for the unsteady cases. For different flows the empirical convergence rates do not necessarily match the expected orders of accuracy. In this paper we have implemented and tested schemes up to fifth order of accuracy in space and time.

We note however, that we have observed difficulties in achieving the fifth order of accuracy for the shallow water equation with source terms. The reasons for this are unclear to us. It could be due to a limitation of the ENO interpolation

procedure. On the other hand the results reported in Appendix B for the model advection-reaction equation suggest that there are not difficulties for the methods proposed in this paper to achieve the desired very high orders of accuracy.

Finally we note that for discontinuous solutions the numerical methods produce essentially non-oscillatory numerical results.

7 APPENDIX A: CAUCHY-KOWALEWSKY PROCEDURE AND ARTIFICIAL SOURCE TERM

System (2) can be rewritten in non conservative form as follows

$$\begin{cases} \frac{\partial h}{\partial t} + \frac{\partial Q}{\partial x} = 0 \\ \frac{\partial Q}{\partial t} + (gD - u^2) \frac{\partial h}{\partial x} + 2u \frac{\partial Q}{\partial x} = -u^2 \frac{\partial b}{\partial x} \end{cases} \quad (16)$$

which can be written in vectorial form as follows:

$$\partial_t \mathbf{U} + \mathbf{A} \partial_x \mathbf{U} = 0 \quad (17)$$

where \mathbf{A} is the matrix:

$$\mathbf{A} = \begin{bmatrix} 0 & 1 \\ gD - u^2 & 2u \end{bmatrix}. \quad (18)$$

In order to solve the derivative Riemann problem we need to express time derivatives in terms of functions of space derivatives using Cauchy-Kowalewsky procedure. To illustrate the method we give time derivatives up to third order:

$$\left\{ \begin{array}{l} \frac{\partial h}{\partial t} = -\frac{\partial Q}{\partial x} \\ \frac{\partial Q}{\partial t} = -(gD - u^2) \frac{\partial h}{\partial x} - 2u \frac{\partial Q}{\partial x} - u^2 \frac{\partial b}{\partial x} \end{array} \right. \quad (19)$$

$$\left\{ \begin{array}{l} \frac{\partial^2 h}{\partial t^2} = u^2 \frac{\partial^2 b}{\partial x^2} + (gD - u^2) \frac{\partial^2 h}{\partial x^2} + 2u \frac{\partial^2 Q}{\partial x^2} \\ \frac{\partial^2 Q}{\partial t^2} = (gD + 3u^2) \frac{\partial^2 Q}{\partial x^2} + 2u^3 \frac{\partial^2 b}{\partial x^2} + 2u (gD - u^2) \frac{\partial^2 h}{\partial x^2} \end{array} \right. \quad (20)$$

$$\left\{ \begin{array}{l} \frac{\partial^3 h}{\partial t^3} = -2u^3 \frac{\partial^3 b}{\partial x^3} - 2u (gD - u^2) \frac{\partial^3 h}{\partial x^3} - (gD + 3u^2) \frac{\partial^3 Q}{\partial x^3} \\ \frac{\partial^3 Q}{\partial t^3} = -4u (gD + u^2) \frac{\partial^3 Q}{\partial x^3} - u^2 (gD + 3u^2) \frac{\partial^3 b}{\partial x^3} - \\ - (gD + 3u^2) (gD - u^2) \frac{\partial^3 h}{\partial x^3} \end{array} \right. \quad (21)$$

8 APPENDIX B: CONVERGENCE RATES FOR LINEAR ADVECTION-REACTION EQUATION

In order to test the accuracy of the ADER numerical method with the ENO reconstruction procedure we have also performed numerical convergence tests

by solving the linear advection reaction equation:

$$\frac{\partial q}{\partial t} + \lambda \frac{\partial q}{\partial x} = \alpha q \quad (22)$$

where λ is the constant wave propagation speed, α is constant reaction coefficient, x is the spatial coordinate and t is time.

Equation (22) have been solved starting from a sinusoidal and a Gaussian initial condition, applying ADER schemes of up fifth order of accuracy in space and time.

Table 6 shows the results. Schemes of order 2 and 4 do not reproduce the expected orders of accuracy, in particular for the L_∞ norm. Odd-order schemes, on the other hand, e.g. orders 3 and 5, reproduce the expected orders of accuracy. We note that for the shallow water equations the second and third order schemes work well even if a Gaussian bed profile is adopted (see Table 3). For the linear advection-reaction equation the odd-order schemes work better.

Table 7 shows the convergence rates for schemes up to fifth order of accuracy, for a test with a Gaussian wave profile as the initial condition. The measured convergence rates do not match the expected ones, for every scheme. The fifth order scheme reproduces the best results.

Acknowledgments. The initial part of this work was carried out while the third author was an EPSRC senior visiting fellow (Grant GR N09276) at the Isaac Newton Institute for Mathematical Sciences, University of Cam-

Table 6

Convergence rates study test for the linear advection reaction equation (22), $\lambda = 1m/s$, $\alpha = -1s^{-1}$ Courant number=0.9, length of the computational domain=1m, results after 2s, initial condition is a sinusoidal wave

Method	N	$L_1 error$	$L_1 order$	$L_\infty error$	$L_\infty order$
ADER 2	10	0.564E-01		0.906E-01	
	20	0.213E-01	1.40	0.448E-01	1.01
	40	0.823E-02	1.37	0.191E-01	1.23
	80	0.273E-02	1.59	0.814E-02	1.23
	160	0.774E-03	1.81	0.335E-02	1.27
ADER 3	10	0.162E-01		0.2504E-01	
	20	0.230E-02	2.81	0.3789E-02	2.72
	40	0.294E-03	2.96	0.4886E-03	2.95
	80	0.370E-04	2.99	0.6132E-04	2.99
	160	0.463E-05	2.99	0.7623E-05	3.00
ADER 4	10	0.600E-02		0.1063E-01	
	20	0.617E-03	3.28	0.1412E-02	2.91
	40	0.482E-04	3.67	0.1641E-03	3.10
	80	0.355E-05	3.76	0.1846E-04	3.15
	160	0.250E-06	3.82	0.2044E-05	3.16
ADER 5	10	0.142E-02		0.2206E-02	
	20	0.471E-04	4.91	0.7664E-04	4.84
	40	0.149E-05	4.97	0.2412E-05	4.98
	80	0.470E-07	4.99	0.7635E-07	4.98
	160	0.147E-08	4.99	0.2392E-08	4.99

bridge, UK, as joint organizer (with P. G. LeFloch and C. M. Dafermos) of the research programme *Non-linear Hyperbolic Waves in Phase Dynamics and Astrophysics*, Cambridge, January to July 2003. The support provided is gratefully acknowledged. The first and second authors acknowledge the support provided by the research project PRIN 2004 *Sviluppo di metodi numerici per applicazioni a problemi di fluidodinamica ambientale*, funded by the Italian

Table 7

Convergence rates study for the linear advection reaction equation (22), $\lambda = 1m/s$, $\alpha = -1s^{-1}$ Courant number=0.9, length of the computational domain=1m, results after 2s, initial condition is gaussian wave with standard deviation $\sigma = 0.2m$

Method	N	$L_1 error$	$L_1 order$	$L_\infty error$	$L_\infty order$
ADER 2	10	0.296E-01		0.672E-01	
	20	0.144E-01	1.034	0.416E-01	0.689
	40	0.534E-02	1.437	0.209E-01	0.992
	80	0.171E-02	1.639	0.941E-02	1.15
	160	0.587E-03	1.544	0.406E-02	1.21
ADER 3	10	0.139E-01		0.356E-01	
	20	0.365E-02	1.929	0.108E-01	1.72
	40	0.607E-03	2.590	0.208E-02	2.37
	80	0.102E-03	2.570	0.283E-03	2.87
	160	0.229E-04	2.154	0.755E-04	1.90
ADER 4	10	0.103E-01		0.273E-01	
	20	0.133E-02	2.949	0.483E-02	2.49
	40	0.180E-03	2.887	0.687E-03	2.81
	80	0.520E-04	1.792	0.177E-03	1.94
	160	0.113E-04	2.193	0.415E-04	2.10
ADER 5	10	0.678E-02		0.179E-01	
	20	0.402E-03	4.076	0.136E-02	3.71
	40	0.103E-03	1.956	0.371E-03	1.87
	80	0.292E-04	1.823	0.175E-03	1.08
	160	0.580E-05	2.333	0.410E-04	2.09

Ministry of Higher Education and Research.

References

- [1] Bermdez A. and Vzquez M. E. Upwind methods for hyperbolic conservation laws with source terms. *Computers and Fluids*, 8:1049.

- [2] L. Bermúdez and M. E. Vázquez. Upwind Methods for Hyperbolic Conservation Laws with Source Terms. *Computers and Fluids*, 23:1049–1071, 1994.
- [3] R. Bernetti, V.A. Titarev, and E. F. Toro. Exact solution of the Riemann problem for the shallow water equations with discontinuous bottom geometry. Technical Report NI06020-NPA, Isaac Newton Institute for Mathematical Sciences, University of Cambridge, UK, 17 May, 2004.
- [4] N Crnjarić-Zić, S. Vuković, and L. Sopta. Balanced finite volume weno and central weno schemes for the shallow water and the open-channel flow equations. *J. Comput. Phys.*, 200, 2004.
- [5] M. Dumbser. *Arbitrary High Order Schemes for the Solution of Hyperbolic Conservation Laws in Complex Domains*. PhD thesis, Institut für Aero- und Gasdynamik, Universität Stuttgart, Germany, 2005.
- [6] M. Dumbser and C. D. Munz. ADER Discontinuous Galerkin Schemes for Aeroacoustics. *Comptes Rendus Mécanique*, –:to appear, 2005.
- [7] L. Fraccarollo and E. F. Toro. A Shock-Capturing Method for Two Dimensional Dam-Break Problems. *Proceedings of the Fifth International Symposium in Computational Fluid Dynamics, Sendai, Japan*, 1993.
- [8] L. Fraccarollo and E. F. Toro. Experimental and Numerical Assessment of the Shallow Water Model for Two-Dimensional Dam-Break Type Problems. *Journal of Hydraulic Research*, 33:843–864, 1995.
- [9] P. Garcia-Navarro and F. Alcrudo. 1d open channel flow simulation using tvd mccormack scheme. *Journal of Hydraulic Engineering, ASCE*,, 118:1359, 1992.

- [10] P. Garcia-Navarro and F. Alcrudo. 1D Open Channel Flow Simulation Using TVD McCormack Scheme. *J. Hydraulic Engineering, ASCE*, 118:1359–1373, 1992.
- [11] S. K. Godunov. Finite Difference Methods for the Computation of Discontinuous Solutions of the Equations of Fluid Dynamics. *Mat. Sb.*, 47:271–306, 1959.
- [12] J. M Greenberg and A. LeRoux. A Well-Balanced Scheme for the Numerical Processing of Source Terms in Hyperbolic Equations. *SIAM J. Numerical Analysis*, 33:1–16, 1996.
- [13] A. Harten, B. Engquist, S. Osher, and S. R. Chakravarthy. Uniformly High Order Accuracy Essentially Non-oscillatory Schemes III. *J. Comput. Phys.*, 71:231–303, 1987.
- [14] M. Käser. *Adaptive Methods for the Numerical Simulation of Transport Processes*. PhD thesis, Institute of Numerical Mathematics and Scientific Computing, University of Munich, Germany, 2003.
- [15] M. Käser. ADER Schemes for the Solution of Conservation Laws on Adaptive Triangulations. *Mathematical Methods and Modelling in Hydrocarbon Exploration and Production*. Springer-Verlag (to appear), 2004.
- [16] M. Käser and A. Iske. Adaptive ADER Schemes for the Solution of Scalar Non-Linear Hyperbolic Problems. *J. Comput. Phys.*, -:-, 2005.
- [17] T. Schwartzkopff. *Finite-Volumen Verfahren hoher Ordnung und heterogene Gebietszerlegung ü die numerische Aeroakustik*. PhD thesis, Institut für Aero-

un Gasdynamik, Universität Stuttgart, Germany, 2005.

- [18] T. Schwartzkopff, Munz C.D, and E. F. Toro. ADER: High-Order Approach for Linear Hyperbolic Systems in 2D. *J. Scientific Computing*, 17:231–240, 2002.
- [19] T. Schwartzkopff, M. Dumbser, and Munz C.D. Fast High-Order ADER Schemes for Linear Hyperbolic Equations. *J. Comput. Phys.*, 197:532–539, 2004.
- [20] C. W. Shu. Essentially Non-oscillatory and Weighted Non-oscillatory Schemes for Hyperbolic Conservation Laws. Technical Report ICASE Report No. 97-65, NASA, 1997.
- [21] Y. Takakura and E. F. Toro. Arbitrarily Accurate Non-Oscillatory Schemes for a Non-Linear Conservation Law. *J. Computational Fluid Dynamics*, 11(1):7–18, 2002.
- [22] V. A. Titarev and E. F. Toro. ADER: Arbitrary High Order Godunov Approach. *J. Scientific Computing*, 17:609–618, 2002.
- [23] V. A. Titarev and E. F. Toro. ADER schemes for shallow water equations with pollutant transport. In *XXIX Convegno di Idraulica e Costruzioni Idrauliche. Trento, Italia, 7-10, Settembre 2004*, pages 909–914. Editorial Bios, 2004.
- [24] V. A. Titarev and E. F. Toro. ADER Schemes for Three-Dimensional Hyperbolic Systems. *J. Comput. Phys.*, 204:715–736, 2005.
- [25] E. F. Toro. Application of the Weighted Average Flux Method to the Shallow Water Equations. In B. Engquist and B. Gustafsson, editors, *Proceedings of the 3rd International Conference on Hyperbolic Problems.*, volume 2, pages 874–887. Chartwell-Bratt, 1991.

- [26] E. F. Toro. Riemann Problems and the WAF Method for Solving Two-Dimensional Shallow Water Equations. *Phil. Trans. Roy. Soc. London*, A338:43–68, 1992.
- [27] E. F. Toro. *Shock-Capturing Methods for Free-Surface Shallow Flows*. Wiley and Sons Ltd, 2001.
- [28] E. F. Toro and Titarev V. A. Derivative Riemann Solvers for Systems of Conservation Laws and ADER Methods. *J. Comput Phys.*, 212(1):150–165, 2006.
- [29] E. F. Toro, R. C. Millington, and L. A. M. Nejad. Towards Very High-Order Godunov Schemes. In *Godunov Methods: Theory and Applications. Edited Review, E. F. Toro (Editor)*, pages 905–937. Kluwer Academic/Plenum Publishers, 2001.
- [30] E. F. Toro and V. A. Titarev. Solution of the Generalised Riemann Problem for Advection-Reaction Equations. *Proc. Roy. Soc. London A*, 458:271–281, 2002.
- [31] E. F. Toro and V. A. Titarev. ADER Schemes for Scalar Hyperbolic Conservation Laws with Source Terms in Three Space Dimensions. *J. Comput. Phys.*, 202(1):196–215, 2005.
- [32] M. E. Vázquez-Cendón. Improved Treatment of Source Terms in Upwind Schemes for the Shallow Water equations in Channels with Irregular Geometry. *J. Comput. Phys.*, 148:497–526, 1999.
- [33] J.G. Zhou, D.M. Causon, C.G. Mingham, and D.M. Ingram. The surface gradient method for the treatment of source terms in the shallow-water

equations. *J. Comput. Phys.*, 168:1, 2001.

[34] C. Zoppou and S. Roberts. Explicit Schemes for Dam-Break Simulations.

ASCE, J. Hydraulic Engineering, 129 (1):11–34, 2003.